ELSEVIER

Journal of Power Sources 81–82 (1999) 273–276

JOURNAL OF POWER SOURCES

www.elsevier.com/locate/jpowsour

Electrochemical properties of sol–gel $Li_{4/3}Ti_{5/3}O_4$

S. Bach [a,*], J.P. Pereira-Ramos [a], N. Baffier [b]

[a] *CNRS UM 7582, Electrochimie, Catalyse et Synthèse Organique, 2 rue H. Dunant, 94320 Thiais, France*
[b] *ENSCP, CNRS URA 1466, Chimie Appliquée de l'Etat Solide, 11 rue P. et M. Curie, 75231 Paris Cedex, France*

Abstract

The synthesis of a mixed lithium titanium spinel $Li_{4/3}Ti_{5/3}O_4$ obtained via a sol–gel process in non aqueous media is reported. The electrochemical behaviour of the sol–gel $Li_{4/3}Ti_{5/3}O_4$ spinel oxide is examined. A voltage plateau located at 1.55 V corresponds to the reversible insertion of 0.95 lithium ions in this compound while the structure is shown to be unchanged. The chemical diffusion coefficient of lithium has been evaluated by a.c. impedance: D_{Li} is found equal to 3×10^{-12} cm^2 s^{-1} for $x = 0.2$ in $Li_{(4/3+0.2)}Ti_{5/3}O_4$.

Keywords: Electrochemical properties; Sol–gel; $Li_{4/3}Ti_{5/3}O_4$

1. Introduction

Chemical and electrochemical studies [1–3] have shown that various titanium oxides can incorporate lithium in different ratios. Brookite and rutile insert only small amounts of lithium, while the anatase form and the synthetic polymorph TiO_2 (B) [4] react extensively with stoichiometries up to 0.8–1 Li per Ti. Therefore many papers are mainly devoted to electrochemical performances of the TiO_2 oxide [5,6]. In particular, the particle size dependence of TiO_2 electrodes [6] as well as the synthetic methods or precursors used for preparing TiO_2 have been shown to strongly influence their electrode performance [7]. Other compounds with a spinel-type structure and corresponding to the spinel oxides $LiTi_2O_4$ and $Li_{4/3}Ti_{5/3}O_4$ have been evaluated in rechargeable lithium cells with promising features [8–11]. In particular, this latter exhibits the best behavior and reversibly inserts 0.7–1 Li per mole of oxide at 1.55 V leading to a specific capacity of 120–150 Ah kg^{-1} after 100 cycles [10].

We have demonstrated the interest in using the sol–gel process for preparing high performance rechargeable cathodic materials especially vanadium and manganese oxides. In this paper, we report the main electrochemical features achieved for the spinel $Li_{4/3}Ti_{5/3}O_4$ synthesized via a sol–gel process.

2. Experimental

2.1. Synthesis of the spinel compound $Li_{4/3}Ti_{5/3}O_4$ [12]

Titania sol–gel synthesis has been developed from the hydrolysis and condensation of metal-organic precursors or metal alkoxides, $Ti(OR)_4$, which indicates they are the result of a direct combination of a metal M with an alcohol ROH. The reactions, traditionally considered with these precursors are those of hydrolysis (Eq. (1)) and of polymerization–condensation by dehydration (Eq. (2)) [10–12].

$$Ti(OR)_4 + H_2O \rightarrow Ti(OH)(OR)_3 + ROH \quad (1)$$

$$\equiv Ti{-}OH + HO - Ti \equiv \rightarrow \equiv Ti{-}O{-}Ti \equiv + H_2O \quad (2)$$

The evolution produces directly a polymeric macromolecule called polymeric gel. Alternatively, for the synthesis of the spinel $Li_{4/3}Ti_{5/3}O_4$, the water molecules are generated in situ by the dissolution of a hydrated lithium salt in alcoholic solvent.

* Corresponding author. Fax: +33-1-4978-1323

0378-7753/99/$ - see front matter
PII: S0378-7753(98)00216-X

Titanium isopropoxide, $[Ti(OCH(CH_3)_2)_4]$ (Aldrich) (0.082 mol) was added to a solution containing $[LiC_2H_3O_2, 2H_2O]$ in 75 ml of ethanol. The resulting yellow solution becomes more and more viscous yielding the formation of a white monolithic gel after 1 h. The gel is dried in air at 60°C during 1 day.

From literature data [13–17], the overall reaction can be written:

$$a\left[Ti(OCH(CH_3)_2)_4\right] + b\left[Li(OAc), 2H_2O\right] \xrightarrow{-(CH_3)_2CHOH} \left[\left[\begin{array}{c} O \\ | \\ O-Ti- \\ | \\ O \end{array}\right]_a O \left[\begin{array}{c} O \\ | \\ -Li- \\ | \\ O \end{array}\right]_b\right]_{Gel}$$

After calcination of the gel, the samples were characterized by X-ray diffraction performed with a Inel diffractometer using the CuKα radiation.

2.2. Electrochemical measurements

The electrochemical measurements were performed in propylene carbonate, twice distilled, obtained from Fluka and used as received. Anhydrous perchlorate was dried under vacuum at 200°C for 12 h. The electrolytes were prepared under a purified argon atmosphere.

The working electrode consisted of a stainless steel grid with a geometric area of 0.5 cm^2 on which the lithium titanium oxide ($\approx$ 5 mg), mixed with graphite (20% by weight), was pressed. Lithium was used as the reference and auxiliary electrodes. Galvanostatic and voltammetric experiments have been performed in a three-electrode cell. Impedance spectroscopy was carried out in the frequency range 10^4–10^{-3} Hz by using an EG and G (PAR) Model 273 A potensiostat coupled with a 1255 Schlumberger frequency-response analyzer. The excitation signal on the system at the equilibrium potential was 10 mV peak to peak. The equilibrium potential was considered to be reached when the drift in open-circuit voltage remained less than 1 mV for 2 h.

3. Results and discussion

The cyclic voltammetric curves for a sol–gel $Li_{4/3}Ti_{5/3}O_4$ electrodes is shown in Fig. 1. One reduction and oxidation processes appear, characterized by the corresponding cathodic and anodic peak potentials respectively

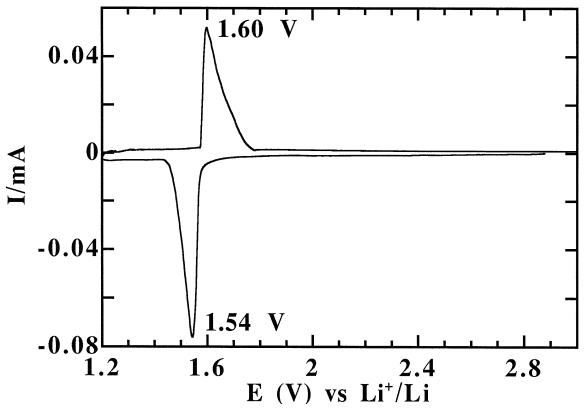

Fig. 1. Cyclic voltammetric curves of a sol–gel $Li_{4/3}Ti_{5/3}O_4$ electrodes in 1 M $LiClO_4$/PC. The scanning rate is 10 $\mu V\ s^{-1}$.

located at 1.54 V and 1.6 V. At a scanning rate of 10 $\mu V\ s^{-1}$ the difference between the cathodic and anodic peak potentials is about 60 mV. Unlike the reduction peak, the shape of the anodic peak current is not symmetric.

The evolution of the equilibrium potential vs.. x in $Li_{(4/3+x)}Ti_{5/3}O_4$ is reported in Fig. 2. From an initial potential of 3 V for the compound without Li, the equilibrium potential sharply decreases with the first all Li ions before to stabilize from the composition $x \approx 0.1$ at 1.56 V. The OCV curve vs. x is constant in the Li composition range $0.1 \leq x \leq 0.8$ which reflects in a first approach a two-phase region. This curve slightly decreases from 0.9 before to drop at $x \approx 0.95$. This contrasts with the open circuit voltage experiments reported for Li insertion in $Li_{2.29}Ti_{3.43}O_8$ [18]. Indeed, they produce different regions characterized by significant dE/dx slopes.

Thus a theoretical specific capacity of 150 Ah kg^{-1} is expected from the maximum uptake of 0.95 per mole of spinel oxide.

This indicates that only 50% of titanium are reduced due to the limited number of available 16 c octahedral sites in the spinel structure of $Li^{8a}[Li^{16d}_{1/3}Ti^{16d}_{5/3}]O_4$ [9,10].

The Li uptake near 0.6 per Ti available near 1.56 V is higher than that achieved for $LiTi_2O_4$ with a maximum value of 0.5 Li/Ti at a lower voltage (1.4 V). A recent work reports a value of 0.7 Li/Ti for electrochemical lithium intercalation in the ramsdellite-type structure $Li_2Ti_3O_7$, i.e., ($Li_{2.29}Ti_{3.43}O_8$) at 1.4 V [18].

From powder X-ray diffraction (Fig. 3), it can be seen that the structure of $Li_{(4/3+x)}Ti_{5/3}O_4$ is practically unchanged as Li accommodation proceeds since the typical diffraction pattern of the parent oxide is recovered, even at a high depth of discharge. For instance at $x = 0.9$, the spinel structure is maintained with only a negligible change in the cubic lattice parameter from 8.344 to 8.357 Å. It should be noted that this is in good agreement with the lattice constants of $Li_{(4/3+x)}Ti_{5/3}O_4$ sample ($0 < x < 0.9$) reported by Ohzuku et al. [10], with $a = 3.37$ Å.

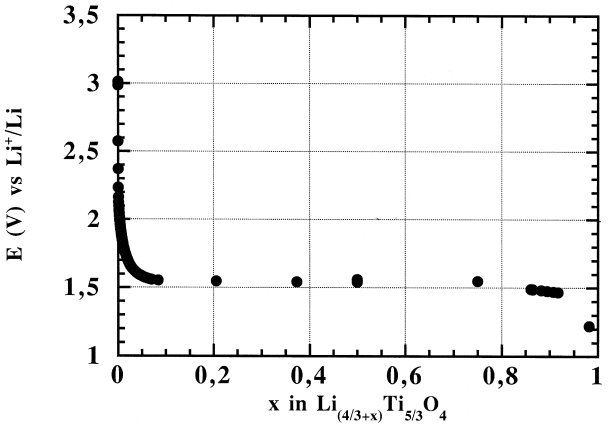

Fig. 2. EMF vs. composition curve for electroformed $Li_{(4/3+x)}Ti_{5/3}O_4$ at 20°C.

Such a result raises an important question on the meaning of a voltage plateau in OCV curve which would rather suggest a two-phase region and X-ray diffraction measurements showing a topotactic insertion reaction without structural change in the spinel oxide.

Fig. 4 displays the chronopotentiometric behaviour of $Li_{4/3}Ti_{5/3}O_4$ at constant current density. At C/60 rate, one main process located at 1.55 V is evidenced and corresponds to the insertion of 1 Li per mole of oxides. Of interest is to note the discharge and charge curves occur at close voltages showing a reversible reaction.

However, for $x < 0.5$ (Fig. 4c,d), the higher the depth of discharge, the lower the efficiency (Q_{ox}/Q_{red}) of the insertion redox process in the spinel structure which reaches a minimum value of 88%. For $x > 0.5$ (Fig. 4 a,b), the initial loss of capacity in the oxidation process no more increases, leading to an efficiency of 94% for the maximum Li uptake. The quantitative extraction of Li from the octahedral 16c sites seems to be hard whatever the depth of discharge. The poor electrical conductivity of the material cannot be completely discarded to explain these results which call for significant improvements in terms of working electrode technology.

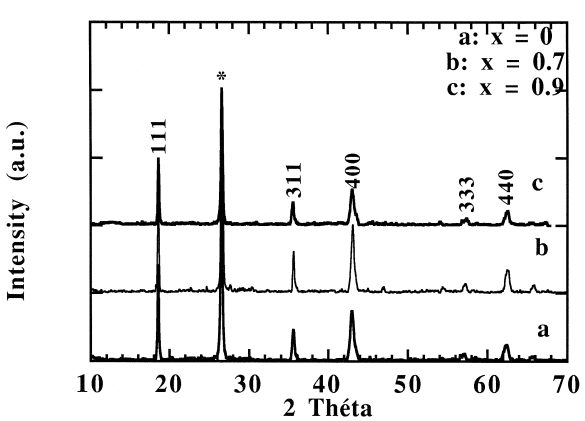

Fig. 3. Evolution of X-ray diffraction patterns as a function of x in electrochemically lithiated $Li_{(4/3+x)}Ti_{5/3}O_4$ samples; (a) $x = 0$, (b) $x = 0.7$; (c) $x = 0.9$. * corresponds to the peak of graphite.

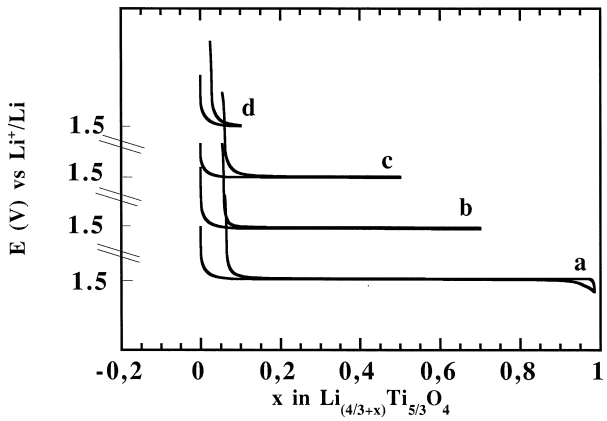

Fig. 4. Chronopotentiometric behaviour of $Li_{4/3}Ti_{5/3}O_4$ as a function of the depth of discharge in 1 M $LiClO_4$/PC (C/60); (a) $\Delta x = 0.1$; (b) $\Delta x = 0.5$; (c) $\Delta x = 0.7$; (d) $\Delta x = 1$.

The lithium intercalation process in cathode generally involves a rate determining step involving solid-state diffusion of Li ions within the cathodic material. Therefore, we have evaluated the kinetics of the Li transport in the $Li_{(4/3+x)}Ti_{5/3}O_4$ using a.c. impedance spectroscopy. A typical complex impedance diagram obtained in the frequency range 10^4–10^{-3} Hz for $Li_{(4/3+0.2)}Ti_{5/3}O_4$ is reported Fig. 5. An important point displayed by Fig. 5 consists in the conventional response obtained as expected for single phase behaviour [19], in good accord with structural experiments. In the high frequency range (10^4–10 Hz) an ill-defined semicircle is obtained for the charge transfer. The porous character of the electrode area is the reason the shape is not a perfect semicircle. According to Fig. 5 in the low frequency range (10^{-1}–2.10^{-3} Hz) a straight line with a slope close to 45° on the real axis is obtained, which corresponds to the Warburg impedance [19]. The Warburg region from which the numerical values of D_{Li} are calculated [19] using Eq. (1) corresponds to a

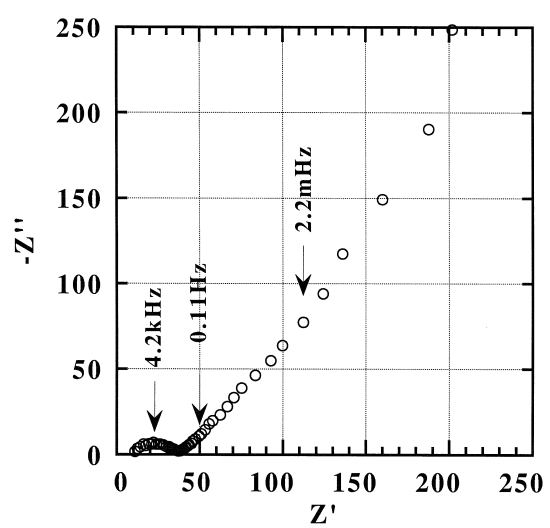

Fig. 5. Typical complex impedance diagram of $Li_{(4/3+x)}Ti_{5/3}O_4$; Frequency range 10^4–10^{-3} Hz ($x = 0.2$).

frequency range where the kinetics of the system is almost entirely limited by the rate of the chemical diffusional process in the host material.

$$D_{Li} = \frac{1}{2}\left[\left(\frac{V_m}{FSA}\right)\left(\frac{dE}{dx}\right)\right]^2 \quad (3)$$

A is obtained from the Warburg impedance ($Z_w = A\omega^{-1/2} - JA\omega^{-1/2}$), $\omega = 2\pi f \gg 2D/L^2$, V_m is the oxide molar volume (21 cm^3), F the Faraday constant, S is the geometric surface area (1 cm^2), dE/dx is the slope of the coulometric titration curve (10^{-2} V). D_{Li} is found to be equal to 3×10^{-12} cm^2 s^{-1} for $x = 0.2$. This apparent value for Li diffusivity in $Li_{(4/3+0.2)}Ti_{5/3}O_4$, is lower than that obtained in the 4 V spinel manganese oxide $LiMn_2O_4$ (10^{-10}–10^{-11} cm^2 s^{-1}).

The main features of Li intercalation in the spinel oxide make this material very attractive as rechargeable cathodic or anodic material characterized by a working voltage of 1.55 V, a specific capacity of 150 Ah kg^{-1} and a diffusivity for Li ions of 3×10^{-12} cm^2 s^{-1}. Due to the electrically insulating character of the initial compound, the optimization of the electrode technology is under investigation to improve the efficiency of the redox process and the cycle life.

Moreover, a deeper investigation of structural, morphological and electrochemical properties is required to answer the existence of a single phase or two-phase mechanism and to elucidate the decrease in capacity [12].

References

[1] T. Ohzuku, T. Hirai, Electrochim. Acta 27 (1982) 1263.
[2] M.S. Whittingham, M.B. Dines, J. Electrochem. Soc. 124 (1997) 1387.
[3] D. Bi, J. Wang, Y. Sun, Z. Liao, Proc. Electrochem. Soc. 80 (1980) 245.
[4] G. Nuspl, K. Yoshizawa, T. Yamabe, J. Mater. Chem. 7 (1997) 2529.
[5] T. Ohzuku, T. Kodama, T. Hirai, J. Power Sources 14 (1985) 261.
[6] S.Y. Huang, G. Campet, N. Treuil, J. Porter, K. Chhor, Active and Passive Elec. Comp. 19 (1996) 189.
[7] Y. Yagi, M. Hibino, T. Kudo, J. Electrochem. Soc. 144 (1997) 12.
[8] E. Ferg, R.J. Gummow, A. de Kock, J. Electrochem. Soc. 141 (1994) L147.
[9] K.M. Colbow, J.R. Dahn, R.R. Haering, J. Power Sources 26 (1989) 397.
[10] T. Ohzuku, A. Ueda, N. Yamamoto, J. Electrochem. Soc. 142 (1995) 1431.
[11] T. Ohzuku, A. Ueda, N.Y. Yamamoto, Y. Iwakoshi, J. Power Sources 54 (1995) 99.
[12] S. Bach, J.P. Pereira-Ramos, N. Baffier, J. Mater. Chem. 8 (1998) 251.
[13] J. Livage, M. Henry, C. Sanchez, Prog. Solid State Chem. 18 (1988) 259.
[14] J. Livage, J. Solid State Chem. 64 (1986) 322.
[15] J.E. Mark, Heter. Chem. Rev. 3 (1996) 307.
[16] K.S. Mazdiyasni, Ceramics International 8 (1982) 42.
[17] H. Dislich, E. Hussmann, Thin Solid Films 77 (1981) 129.
[18] M.E. Arroyo y de Dompablo, E. Moran, A. Varez, F. Garcia-Alvarado, Mater. Res. Bull. 32 (1997) 993.
[19] C. Ho, I.D. Raistrick, R.A. Huggins, J. Electrochem. Soc. 127 (1980) 343.